Original article

Findings of Cardiac Radionuclide Images in Myotonic Dystrophy*

Norinari Honda, MD, Kikuo Machida, MD, Makoto Hosono, MD, Hajime Toyoda, MD, Masanobu Kinoshita**, MD, Yusuke Inoue†, MD, Taku Takahashi, MD, Tsuyoshi Kamano, MD, Akio Kashimada, MD, and Hisato Osada, MD

Department of Radiology and **Department of Internal Medicine IV, Saitama Medical Center, Saitama Medical School

Abstract

Purpose of this study was to report our experiences of cardiac radionuclide imaging in patients with myotonic dystrophy to assess its clinical implications. Consecutive 18 patients (6 men and 12 women with age range of 34 - 66 years) entered the study. Thallium-201, I-123 BMIPP, and I-123 MIBG myocardial SPET were performed 15 minutes and 195 minutes after the injection of the radiotracers (111 MBq). SPET images were interpreted by consensus of 3 nuclear medicine physicians blinded to clinical information. Bull's eye washout rates of SPET of the three rediopharmaceuticals, H/M ratios of I-123 MIBG planar images were calculated. Reduced uptake was found in 93 and 103 out of 234 segments on early and delayed Tl-201 SPET, 110 and 104 out of 234 on I-123 BMIPP, and 71 and 81 out of 221 on I-123 MIBG, respectively. The photopenia was mild in majority. Frequency of photopenic areas was greater in I-123 BMIPP than in Tl-201 ($p = 0.001$) followed by I-123 MIBG ($p < 0.0001$). Photopenia was most often found in infero-posterior wall ($p < 0.0001$). The washout rates and H/M ratios between mild and severe disease were not statistically different after excluding the patients complicated with diabetes mellitus. In conclusion, radionuclide myocardial imaging is frequently abnormal in the patients with myotonic dystrophy. Early detection of the cardiac involvement may be possible in some patients by cardiac radionuclide imaging.

Key words: heart, myotonic dystrophy, SPET, MIBG, BMIPP (223 words excluding the key words)

Introduction

Myotonic dystrophy is a hereditary disease with variegated signs and symptoms including myotonia, muscle atrophy and weakness, gonadal dysfunction, baldness, cataract, and mental retardation [1,2]. Cardiac muscle is also involved in the disease. The involvement is characterized pathologically by fatty infiltration and scattered fibrosis [3]. It rarely causes cardiac failure [2], but frequently leads to sudden deaths. The sudden death, probably related to cardiac conduction abnormality [1,3,4], constitutes about 30% of all death of patients with this disease [3]. Thus, early detection of cardiac involvement is mandatory for predicting prognosis, or preventing the sudden death with appropriate means.

Branched chain fatty acid, I-123-beta-methyliodophenylpentadecanoic acid (I-123 BMIPP) and catecholamine analogue, I-123-metaiodobenzylguanidine (I-123 MIBG), are tend to show more extensive photopenia than Tl-201 in ischemic heart disease and cardiomyopathy [5-13]. We also experienced a patient with myotonic dystrophy, who showed a area of decreased I-123 MIBG uptake despite normal Tl-201 myocardial accumulation in the area [14]. We speculated that I-123 BMIPP and I-123 MIBG cardiac imaging may be more sensitive than other modalities in patients with myotonic dystrophy. Purpose of this study was to report our experiences with these radiotracers to assess their clinical implications.

Contact address :
1981 Tsujido, Kamoda, Kawagoe, Saitama 350-8550, Japan Norinari Honda, MD
TEL. 81-49-225-781 1 FAX. 81-49-226-5274

Genetic basis of myotonic dystrophy has been established recently. The gene encoding a protein called myotonin protein kinase [15-16] has elongated cytosine-thymine-guanine (CTG) triplet repeats. The degree of the CTG-repeat expansion is correlated with the increasing severity of the disease [15-16]. Therefore, we classified the patients into mild and severe disease by the CTG repeat length in leukocytes.

Methods

Patients

There were 18 consecutive patients with myotonic dystrophy diagnosed at the authors' institution from January 1992 through December 1995. These eighteen patients constituted a study population. There were 6 men and 12 women with age range of 34 to 66 years (mean ± SD; 49 ± 10 years). The diagnosis of myotonic dystrophy was made by a neurologist (M. K.) with characteristic physical findings including percussion myotonia, muscle weakness, and other signs and symptoms.

The patients' profiles are included in **Table 1**. All the patients did not have any symptoms and signs of cardiac failure though two-dimensional echocardiography revealed mild, generalized hypokinesia in 4 patients, and aortic regurgitation in 1 patient. Non-insulin dependent diabetes mellitus (NIDDM), pseudohypoparathyroidism type 2 (PHP2), and gall bladder stone (GBS), Sjogren syndrome (SjS), were complicated in 6, 4, 2, and 1 of the patients, respectively. Cardiac pacemaker (CPM) was implanted in 1 patient because of cardiac syncope. One patient died suddenly 7 months after the cardiac imaging study.

All of the radiopharmaceuticals is approved for clinical use by the Government of Japan. Informed consent was obtained from all the patients.

Gene analysis

Standard Southern blot analysis was utilized to investigate the degree of the CTG-triplet repeats as described previously [17]. Briefly, Genomic DNA of 10 μg was extracted from the peripheral white blood cells of the patients and was digested by a restriction enzyme, EcoR I. The digested DNA was transferred onto nitrocellulose membranes after electrophoresis on 0.7% agarose gel. The sample was then hybridized with a P-32-labeled cDNA25 probe. Blots were exposed to X-ray film for 1 to 14 days at -80℃.

Size of the expanded fragment on the blot was used to classify the patients with mild and severe disease: patients with the fragments smaller or equal to 13 kilobases (kb) were classified as mild and those with the fragments larger than 13 kb as severe disease.

Radionucljde Imaging protocol

Thallium-201 (Daiichi Radioisotope Laboratories, Tokyo; or Nihon Mediphysics, Takarazuka), I-123 BMIPP (Nihon Mediphysics, Takarazuka), and I-123 MIBG (Dailchi Radioisotope Laboratories, Tokyo), each in a dose of 111 MBq, were injected intravenously on separate occasions to each of the patients after an overnight abstinence from food and their drugs. Cardiac drugs and anti-depressants were not taken by any of them. The patients were instructed to keep the abstinence till the end of each study except for water. Lugol's solution of 1 ml/day, or potassium iodide of 100 mg/day, was administered orally for 5 days beginning from 2 days before the injection of I-123 BMIPP and I-123 MIBG. Thallium-201 was injected 6 minutes after the start of dipyridamole infusion (0.56 mg/kg in 4 minutes) coupled with a 4-minute handgrip exercise starting from the end of the dipyridamole infusion. I-123 BMIPP and I-123 MIBG were injected at rest.

Data acquisition of SPET of the heart was performed twice, early and delayed, for each of the radiopharmaceuticals. The early and delayed SPETs were started 15 and 195 minutes after the injection of the radiopharmaceuticals. A three-detector SPET system equipped with low-energy, general-purpose, parallel-hole collimators (Prism 3000, Picker, Cleveland) was employed. A photopeak was centered on 70 keV with window width of 20% for Tl-201, and 159 keV with 20% window width for I-123. Total of 72 views was acquired for 30 seconds/view for Tl-201 and I-123 BMIPP, or 45 seconds/view for I-123 MIBG, on a 64x64 matrix during a 360-degree rotation in a

step-and-shoot fashion. Voxel size was 5.34 mm. A single-detector SPET system (SNC 510R, Shimadzu, Kyoto) equipped with a low-energy, parallel-hole, all-purpose collimator was used in 3 patients (Case 1, 6, and 11). Data acquisition parameters for this camera were the same as above except for a 180-degree arc from right anterior oblique 45° to left posterior oblique 45°, and 32 projection images.

Additional anterior planar I-123 MIBG scintigrams of the thorax were acquired 5 minutes before the start of SPET with the same imaging system with an imaging matrix of 256 x 256 (pixel size = 1.3mm) and imaging time of 3 minutes.

All the three imaging studies were performed within 3 weeks except in 3 patients (**Table 1,** 2 months in case 8, 12 months in case 4, and 20 months in case 14). The three patients were clinically stable without marked progression of their symptoms and signs during the intervals.

Transverse images were reconstructed by filtered (Ramp filter) back projection without attenuation correction after Butterworth pre-filtering (order 4, cutoff 0.23-0.28 cycle/pixel with visual optimization). Short axis, and vertical and horizontal long axis views of left ventricles were reoriented from stacks of the transverse images encompassing the entire heart.

Data acquisition and image reconstruction, as well as image analysis described below, were performed on the dedicated computers connected to the gamma cameras with the computer programs supplied by the camera vendors.

Image interpretation

Three nuclear medicine physicians visually interpreted the cardiac 3-plane SPET images by consensus on 3-grade defect scale (normal, reduced uptake, defect) and assigned the photopenias or defects to corresponding segments of **Figure. 1** without clinical information except for patients' age and gender. The image interpretation sessions were separately held for each of radiopharmaceuticals without referral to the image sets of the other radiopharmaceuticals. Two SPET examinations were excluded because the physicians judged image quality was so poor to preclude valid image interpretation **(Table 1)**.

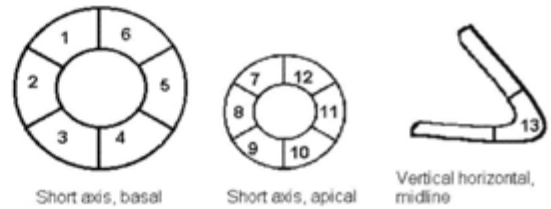

Figure 1. Definition of segments.

Image analysis

Qualitative image analysis was made only in 12 patients after excluding the six patients complicated with NIDDM because the disease is reported to affect I-123 MIBG washout [18]. Bull's eye washout rate maps of Tl-201, I-123 BMIPP and I-123 MIBG were created from sets of circumferential profiles of early and delayed short axis images encompassing the heart except for the apex. Each of the circumferential profiles was composed of the maximum pixel count in each of the sixty sectors created by radial division of a short axis image. Washout rates were enumerated by dividing differences in the corresponding profile values by the values of the early images after physical decay correction. Mean washout rates were calculated from these values.

Regions of interest (ROIs) were placed at the upper mediastinum (fixed size rectangular, 6 x 12 horizontal x vertical pixels) and encircling the heart (manually drawn, variable size) on an anterior planar I-123 MIBG scintigrams. H/M ratio and washout rate were calculated from mean pixel values of the ROIs with physical decay correction [18].

Electrocardjography and echocardiography

Electrocardiography (ECG) and echocardiography were performed within 1 week of the start or the completion of the cardiac radionuclide studies. They were analyzed and interpreted by cardiologists in the authors' hospital. Standard 12-lead electrocardiography was recorded at rest. Ambulatory 24-hour electrocardiography was recorded continuously on a cassette tape (SM50, Fukuda Denshi, Tokyo) followed by computer analysis of arrhythmia and ST-T changes. Two-dimensional echocardiography was performed

Table 1. Imaging and clinical profiles of the patients*

				No. of photopenic segments						Washout rate, %				H/M ratio	
	Age		SEF	Tl		BMIPP		MIBG		SPET			Planar	Planar	
No.	yr	G	kb	E	D	E	D	E	D	Tl	BMIPP	MIBG	MIBG	E	D
1	66	F	10.0	4	4	4	7	3	6	55	22	35	29.2	2.56	2.46
2	34	F	11.1	3	3	4	5	5	5	25	28	1	22.9	2.17	2.35
3	34	M	11.4	10	10	9	11	5	7	43	36	14	21.6	3.19	3.22
4	45	F	11.4	6	6	4	4	4	5	47	25	9	17	2.51	2.79
5	40	F	11.5	3	5	7	7	5	7	58	13	6	4.1	2.60	3.40
6	56	F	11.5	7	7	8	4	2	6	53	0	3	12.7	2.29	2.40
7	57	M	11.5	6	8	7	6	4	4	25	21	17	29.9	2.97	3.15
8	61	M	11.7	9	9	11	10	7	7	31	8	20	31.9	2.20	2.44
9	52	F	12.8	7	7	9	4	8	8	61	7	65	28	2.86	2.97
10	36	F	13.0	10	10	9	12	nd	nd	37	15	nd	56	1.85	1.73
11	54	M	13.2	5	8	7	6	2	5	47	2	8	17.8	2.89	3.04
12	45	F	14.0	13	10	8	13	4	5	30	25	34	45.5	2.35	1.99
13	46	M	14.0	2	4	10	10	10	8	20	0	27	36.2	2.72	2.59
14	58	F	14.6	10	10	4	2	7	8	58	nd	6	29.3	2.63	2.65
15	57	F	14.8	5	6	11	9	6	7	17	23	29	32.8	1.96	2.04
16	31	F	15.2	6	7	nd	nd	8	2	61	-26	16	19.8	2.69	3.18
17	54	M	15.4	9	10	10	10	4	3	39	12	27	32.1	3.27	3.02
18	54	F	15.5	6	7	9	8	6	8	43	10	29	26.9	1.99	2.08

* G: gender, SEF: size of expanded fragments on Southern blot in kilobases (kb), E: early imaging, D: delayed imaging, H/M ratio: heart-to-mediastinum ratio of MIBG, RD: segment number showing redistribution on Tl SPECT, ECG: electrocardiography, LVEF: left ventricular ejection fraction, nd: no data available
† CRBBB: complete right bundle branch block, Af: atrial fibrillation, 1AVB or 2 AVB: I° or II° AV block, LAH: left anterior hemiblock, IVCD: intraventricular conduction delay, PVC: premature ventricular contraction, PAC: premature atrial contraction
‡ AR3: aortic regurgitation grade 3, hypo: global hypokinesia
¶ See text for the abbreviations.

(to be continued)

(SSD 2200, Aloca, Tokyo) and left ventricular ejection fraction (LVEF) was calculated by Gibson's method [19].

Statistical analysis

The number of segments with photopenia or defect was counted. Chi-square test was utilized to test differences of abnormality rates on SPET and ECG. The frequency of photopenic segments including defects was compared by three-way analysis of variance (ANOVA) since the number of the segments differed among the locations or the patients' groups. Factors tested were radiopharmaceuticals and timing of imaging. The third factor was either disease severity or location of photopenia. Fisher's protected least significant difference test was applied as a multiple comparison test after the ANOVA.

Differences of the washout rates (Tl-201, I-123 BMIPP, I-123 MIBG, and I-123 MIBG planar images), H/M ratios of I-123 MIBG (early and delayed), and LVEF were tested between the mild and severe disease by Mann-Whitney U-test. Multivariate discriminant analysis was performed setting the washout rates, H/M ratios, and LVEF as variables, and setting disease status (mild or severe) defined by the size of the expanded fragments as standard.

Two-way ANOVA was used to test the concordance rate between SPET findings of the two radiopharmaceuticals. Chi-square test was utilized to test differences of redistribution, or fill-in, rates. Significance level was set to 0.05 (5%) for all the statistical tests.

Results

The patient profiles and the results of the gene analysis are summarized in **Table 1**. All the patients had an abnormally expanded (greater than 9.6 kb) fragment containing CTG triplet repeats on the Southern blot, which confirmed the clinical diagnosis of myotonic dystrophy.

Photopenic segments were found in all the

Table 1 (continued)

RD	ECG†	24-hour ambulatory ECG	Echocardiography‡ LVEF	wall motion	complication ¶
	CRBBB,Af	186 PVC couplets	0.47	AR3	
	normal	223 PVC couplets	0.69	normal	NIDDM
	normal	no arrhythmia	0.61	normal	
1, 2	1AVB	no arrhythmia	0.54	normal	
	normal	48 PVC couplets, PAC	0.76	normal	
	1AVB	no arrhythmia	0.68	normal	PHP2
3, 5	1AVB	occasional PVC	0.55	mild hypo	NIDDM
4	1AVB	not done	0.64	normal	
	1AVB	124 PAC_S	0.85	normal	PHP2, SjS
	1AVB	no arrhyihmia	0.62	normal	NIDDM
	1AVB	not done	0.45	mild hypo	
	1AVB,LAH	1AVB, PVC	0.46	mild hypo	
	IVCD	no arrhythmia	0.62	normal	PHP2, SD
	1AVB	no arrhythmia	0.54	mild hypo	NIDDM, GBS
	2AVB,SSS	2AVB,PVC	0.66	normal	NIDDM, CPM, GBS
4	normal	no arrhythmia	0.57	normal	
	IVCD	no arrhythmia	0.58	normal	PHP2, GBS
	1AVB	no arrhythmia	0.64	normal	NIDDM, PHP2

Table 2. Summary of cardiac radionuclide imaging*

Group	Radio-pharm**	Early imaging D	R	N	Sum	Delayed imaging D	R	N	Sum
All									
	Thallium	5	88	141	234	4	99	131	234
	BMIPP	3	107	111	221	10	94	117	221
	MIBG	2	69	150	221	1	80	140	221
	Sum	10	264	402	676	15	273	388	676
Group 1 (mild dis.)	Thallium	4	48	78	130	2	55	73	130
	BMIPP	1	59	70	130	3	54	73	130
	MIBG	0	33	84	117	0	44	73	117
	Sum	5	140	232	377	5	153	219	377
Group 2 (severe dis.)	Thallium	1	40	63	104	2	44	58	104
	BMIPP	2	48	41	91	7	40	44	91
	MIBG	2	36	66	104	1	36	67	104
	Sum	5	124	170	299	10	120	169	299

*n = 18. Values are the number of segments. D: defect, R: reduced accumulation, N: normal. Group 1 is composed of the patients with the size of the expanded fragments ≤13 and Group 2 > 13kb on Southern blot analysis.
**Radiopharmaceutical is the only significant factor influencing the frequency [= D + R)/Sum] of photopenia.

patients with all the radiopharmaceuticals. Resting ECG was abnormal in 14 patients, in whom the first-degree atrioventricular block was most frequent. Ambulatory 24-hour ECG showed no arrhythmia in 9 out of 16 patients tested. The occurrence of abnormalities in SPET images were significantly more frequent than that of ECG ($p = 0.034$) or 24-hour ambulatory ECG ($p = 0.016$). Sudden death occurred 7 month after the completion of SPET in case 13, who showed photopenic segments on SPET studies but no arrhythmia on 24-hour ECG **(Table 1)**.

Result of the SPET interpretation is shown in **Table 2**. Photopenia was usually mild. Defects constituted only 1.5% (10/676 segments) on early and 2.2% (15/676) on delayed imaging. The kind of the radiopharmaceuticals was significant factor ($p = 0.0001$), but disease severity and image timing (early vs. delayed imaging) were not significant factors to affect frequencies of photopenia ($p = 0.21$, 0.15, respectively). The frequencies of photopenia were 0.484 (428/884) in I-123 BMIPP, 0.419 (392/936) in

Table 3. localization of photopenia*

Radio-pharm**	LV location**	Early imaging				Delayed imaging			
		D	R	N	Sum	D	R	N	Sum
Thallium	Ant	0	12	24	36	0	20	16	36
	Sep	0	27	45	72	2	24	46	72
	Inf-pos	4	22	10	36	1	27	8	36
	Lat	0	19	53	72	0	20	52	72
	Apex	1	8	9	18	1	8	9	18
	Sum	5	88	141	234	4	99	131	234
BMIPP	Ant	0	13	21	34	0	17	17	34
	Sep	0	35	33	68	5	23	40	68
	Inf-pos	2	24	8	34	3	26	5	34
	Lat	0	27	41	68	1	21	46	68
	Apex	1	8	8	17	1	7	9	17
	Sum	3	107	111	221	10	94	117	221
MIBG	Ant	0	9	25	34	0	5	29	34
	Sep	0	23	45	68	0	18	50	68
	Inf-pos	1	22	11	34	0	27	7	34
	Lat	0	12	56	68	0	24	44	68
	Apex	1	3	13	17	1	6	10	17
	Sum	2	69	150	221	1	80	140	221

*n - 18. Values are the number of segments. D: defect, R: reduced accumulation, N: normal, **Statistically significant two factors affecting the frequency [=(D+R)/Sum] of photopenia. Ant: anterior wall, Sep: septum, Inf-Pos: infero-posterior wall, Lat: lateral wall.

Table 4. Concordance of photopenia*

Early imaging

	BMIPP			
Tl	D	R	N	Sum
D	2	2	1	5
R	0	61	23	84
N	1	44	87	132
Sum	3	107	111	221

	MIBG			
Tl	D	R	N	Sum
D	1	3	1	5
R	1	38	41	80
N	0	28	108	136
Sum	2	69	150	221

	MIBG			
BMIPP	D	R	N	Sum
D	1	1	1	3
R	0	48	52	100
N	1	14	90	105
Sum	2	63	143	208

Delayed imaging

	BMIPP			
Tl	D	R	N	Sum
D	1	2	0	3
R	4	60	30	94
N	5	32	87	124
Sum	10	94	117	221

	MIBG			
Tl	D	R	N	Sum
D	0	2	1	5
R	0	48	44	92
N	1	30	95	126
Sum	1	80	140	221

	MIBG			
BMIPP	D	R	N	Sum
D	0	8	1	9
R	1	47	37	85
N	0	23	91	114
Sum	1	78	129	208

*n = 18. Values are the number of segments. D: defect, R: reduced uptake, N: normal uptake. No statistical differences among the concordance rates.

Tl-201, and 0.344 (304/884) in I-123 MIBG. The frequency was greatest in I-123 BMIPP followed by Tl-201 and I-123 MIBG in decreasing order of frequency ($p = 0.012$ and $p < 0.0001$ in comparison with Tl-201, and $p < 0.0001$ between I-123 BMIPP and I-123 MIBG, respectively).

Distribution of photopenia within the left ventricles is shown in **Table 3**. The location within left ventricles was a statistically significant variable ($p = 0.001$). Overall frequencies of photopenia were 0.774 (124/416) in infero-posterior wall, 0.366 (76/208) in anterior wall, 0.401 (167/416) in septum, 0.298 (124/416) in lateral wall, and 0.442 (46/104) in apex. The infero-posterior wall was the most frequent site ($p < 0.0001$) though there were no differences among anterior wall, lateral wall, septum, and apex ($p > 0.11$).

Concordance of the photopenia is shown **Table 4**.

Table 5. Changes in SPET findings during 3-hour interval*

a) Thallium

		Delayed			
		D	R	N	Sum
Early	D	1	3	1	5
	R	2	70	16	88
	N	1	26	114	141
	Sum	4	99	131	234

b) BMIPP**

		Delayed			
		D	R	N	Sum
Early	D	1	2	0	3
	R	7	64	36	107
	N	2	28	81	111
	Sum	10	94	117	221

c) MIBG

		Delayed			
		D	R	N	Sum
Early	D	1	1	0	2
	R	0	49	20	69
	N	0	30	120	150
	Sum	1	80	140	221

*n = 18. Values are the number of segments. D: defect, R: reduced uptake, N: normal uptake.
**Statistically more frequent fill-in than other radiotracers.

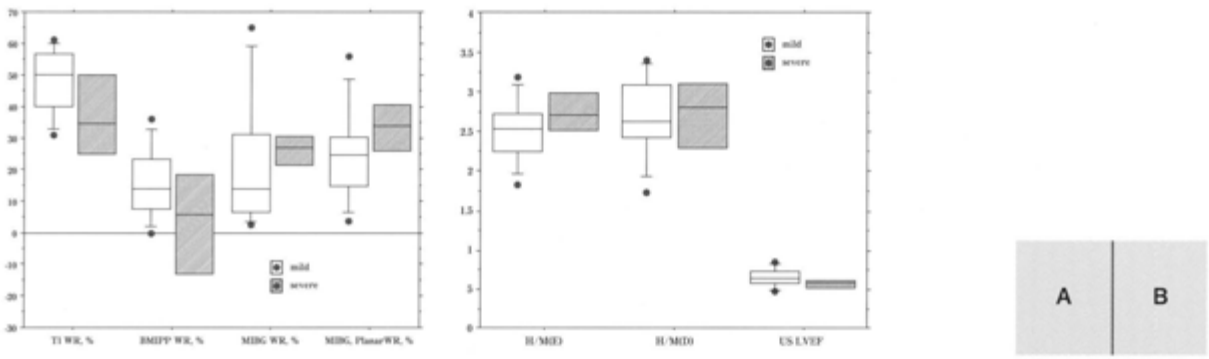

Figure 2.
Comparison of image-derived indices between mild and severe disease. Box plots of the washout rates (A), and H/M ratios and LVEF (B) after the exclusion of the patients complicated with diabetes mellitus show that there are no significant differences in all indices by Mann-Whitney U-test.

Mismatched segments were found in 34%(76/221) of Tl-201, 33%(74/221) of I-123 BMIPP, and 28%(59/208) of I-123 MIBG in the early imaging, while 33%(73/221), 35%(78/221), and 33%(70/208) in the delayed imaging, respectively. There was no statistical significance among these rates ($p > 0.29$). There were all types of mismatches. However, the absent accumulation on one radiotracer with normal or reduced accumulation on the other was seen in less than 4 segments except for the I-123 BMIPP defects with preserved accumulation of the others on delayed imaging (9 segments).

Redistribution or fill-in is shown in **Table 5.** It was found in 8.5% (20/234) on Tl-201, 17% (38/221) on I-123 BMIPP, and 9.5% (21/221) on I-123 MIBG. The frequencies of redistribution, or fill-in, were larger in I-123 BMIPP than in Tl-201 ($p = 0.012$) and I-123 MIBG ($p = 0.017$), both were tied ($p = 0.87$).

The washout rates of Tl-201, I-123 BMIPP, and I-123 MIBG as well as the H/M ratio of I-123 MIBG planar scintigrams were not statistically different between the patients with mild and severe disease ($p > 0.148$, **Figure 2**).

The calculated multivariate linear discriminant function, z, was

$$z = 0.0796WR_{Tl} + 0.3187WR_{BMIPP} + 0.1196WR_{MIBG} - 0.4777WR_{MIBGpl} - 8.5860H/M_E - 2.31921H/M_D + 20.3210LVEF + 20.7395$$

with negative z value denoting severe disease, where WR, H/M, and LVEF are washout rate, H/M ratio, and echocardiographic left ventricular ejection fraction. Subscripts are the name of the radiopharmaceuticals except for E (early), D (delayed), and pl (planar image). The function was not statistically significant ($p = 0.367$).

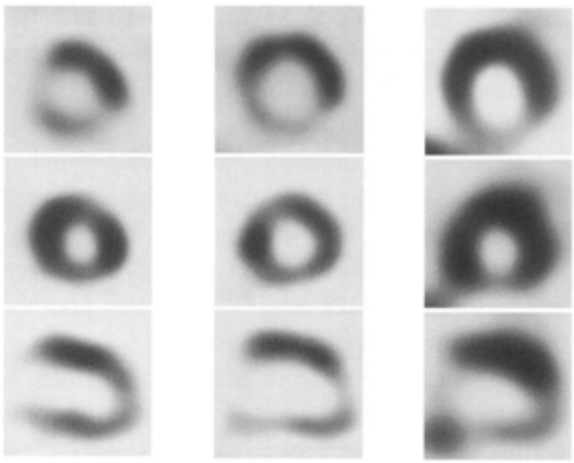

Figure 3.
Myotonic dystrophy, 54 year-old man (case 11). (A) Delayed Tl-201, (B) early ^{123}I-BMIPP SPET, (C) delayed ^{123}I-MIBG SPET. There were photopenic segments at the apex, apical anterior wall, and infero-posterior wall. The photopenia was interpreted as more prominent on ^{123}I-BMIPP than on ^{201}Tl SPET.

A representative case is illustrated in **Figure 3.**

Discussion

Myotonic dystrophy is now recognized as a disease of expanded and unstable cytosine-thymine-guanine (CTG) triplet repeats on a gene [15,16]. Patients with myotonic dystrophy have abnormal CTG triplet repeats on untranslated 3' portion of the gene on chromosome 19, which is coding for myotonin-protein kinase [20]. Length of the triplet repeat is usually correlated with the disease severity, and inversely correlated with the time of the disease onset [15,16]. The length was not directly measured in the study, though it could be estimated from the size of the expanded fragments on a Southern blot analysis [21,22]. The threshold between small and large triplet repeat is 700 [22], which is equivalent to 13kb by the EcoR I digested Southern blot. Disease severity was classified by this threshold of 13 kb in the present study.

Reduced uptake of the radiotracers was noted in all the patients. The frequency was statistically more greater than that of ECG or 24-hour ECG. Thus, radionuclide cardiac imaging may be more sensitive, or may detect the abnornrality earlier in some patients, than ECG. The photopenia was most often seen in I-123 BMIPP SPET. I-123 BMIPP may be the radiopharmaceutical of choice to diagnose the myocardial involvement by the disease if the photopenias are demonstrated to be due to myotonic dystrophy.

Cause of photopenia was not rigorously established in the study. We speculate that photopenia may be due to fibrosis and fatty infiltration of the myocardium reported in this disease[3]. Regional difference of photopenia may reflect regional difference of the fibrosis and fatty infiltration. Coronary artery disease is probably not a cause of the photopenia, since we did not observe photopenia conforming the coronary territory. Coronary angiography was not performed in this study to exclude coronary artery disease. Coronary artery disease was complicated in 4 of 12 patients in Nguyen's study [3]. He did not find any myocardial lesions attributable to coronary artery disease even in the four patients, while he found fibrosis, fatty infiltration, and degeneration in myocardium and conduction system.

Nuclear medicine has been successful in revealing abnormality of myocardium otherwise not apparent. Washout of I-123 MIBG is accelerated in diabetes mellitus [18,23,24] and heart failure [25,26]. The H/M ratio of I-123 MIBG is low in these conditions [18,23-26]. Positron emission tomography with F-18-fluorodeoxy glucose also demonstrated that glucose phosphorylation in the myocardium of myotonic dystrophy decreases with increasing length of the repeats [21]. Accordingly we excluded the patients with NIDDM from the quantitative image analysis, and also expected that the image and the image-derived indices might be different between the patients with mild and severe, or shorter and longer CTG triplet repeats. The

washout rates, and H/M ratios were not significantly different between mild and severe disease in this series. This may mean that these indices do not reflect the disease severity.

The length of the CTG repeats, however, does not always correlate with the disease severity [15,16]. The length of the CTG triplet differs between tissues of an individual [22,27]. There is another possibility that the severity of the cardiac involvement could only be gauged by the CTG triplet expansion of the myocardial DNA, not by leukocytic DNA.

Serial ECG is reported to be useful for defining high risk group for sudden death [28]. Correlation of prognosis and findings on the radionuclide imaging is an important point. However this was not investigated in this study. Demonstration of the correlation needs follow-up and repeated imaging studies.

There were mismatched myocardial segments with normal (or less severe reduction in) Tl-201 uptake and decreased I-123 MIBG uptake. The mismatched I-123 MIBG defects could be explained by sympathetic denervation. The mismatched I-123 MIBG defect is closely correlated with ventricular tachycardia in patients with old myocardial infarction [11] and arrhythmogenic right ventricular disease [29,30]. The uptake of I-123 MIBG is asymmetric in patients with recurrent ventricular tachycardia of "clinically normal heart" [31]. Correlation of arrhythmia and inhomogeneous I-123 MIBG uptake is also reported in long QT syndrome [31]. Sudden death is a leading cause of the death in myotonic dystrophy [3], which is probably due to cardiac arrhythmia [28]. One patient in this series (case 13) succumbed suddenly, in whom the mismatch was found in lateral wall, basal septum, and inferior wall on delayed I-123 MIBG and Tl-201 SPET. Correlation of arrhythmia and I-123 MIBG-Tl-201 mismatch is suggested in this particular patient.

Other types of mismatches were also found. Mismatched I-123 BMIPP defects may be explained by its higher sensitivity for the detection of ischemia [6-9]. The mismatched Tl-201 defects may be explained in part by greater photon attenuation than I-123 because about half of the mismatched defects were found anterior and infero-posterior wall. However, another half could not be explained by the difference of the attenuation. One possible explanation is the variation in the interpretation.

One patient did not accumulate I-123 MIBG in her heart (case 10). This is most reasonably explained by coexisting diabetes mellitus with neuropathy, not by myotonic dystrophy. Cause of the severe inhomogeneous I-123 BMIPP uptake in another patient (Case 16) was not elucidated.

Care must be exerted in interpreting defects in the infero-posterior wall and anterior wall. There is normal inhomogeneity of I-123 MIBG distribution [33-35]. Defects in the infero-posterior wall may be artifacts due to diaphragmatic attenuation of gamma rays. Anterior wall defect on Tl-201 imaging may be due to attenuation from large breasts. High count in the liver attaching or near the infero-posterior wall causes artificial defect in the infero-posterior wall [36]. We visually interpreted the images keeping the normal inhomogeneity and potential sources of artifacts in mind because normal database was not available. This is another limitation of this study.

Multivariate discriminant analysis apparently showed that only the indices obtained from I-123 MIBG had negative coefficients suggesting I-123 MIBG as the most effective radiotracer to discriminate severe and mild disease. However, this could not be ascertained in the present study since the function was not significant.

Conclusion

Radionuclide myocardial imaging was invariably abnormal in the patients with myotonic dystrophy in this series. The prevalence of the abnormality was higher than that of ECG suggesting some clinical value of the imaging. Photopenia was most often seen in the infero-posterior wall. The prevalence of photopenia was significantly greater on I-123 BMIPP followed by Tl-201 and I-123 MIBG. Washout rates of Tl-201, I-123 BMIPP, and I-123 MIBG as well as H/M ratio of I-123 MIBG were not different between the patients with shorter and longer cytosine-thymine-guanine triplet repeats after excluding the patients with diabetes mellitus.

Acknowledgement

A part of this investigation was supported by the grant of Japanese Ministry of Ednealim (No 10670869, 08671048, 06670933) The authors thank Ryosuke Miyano, NMT, Satoshi Kobayashi, NMT, and other staffs of the Department of Radiology for their technical assistance. Part of this study was presented at the annual meeting of the European Association of Nuclear Medicine, Copenhagen, September 14-18, 1996.

References

1. Wenger NK, Goodwin JF, Robbers WC: Cardiomyopathy and myocardial involvement. In: Hurst JW, Longue RB, Rackley CE, Schlant RC, Sonnenblick EH, Wallace AG, Wenger NK (eds): The heart, 6th edition. New York, McGraw-Hill, 1986, pp1230-1230.
2. Mendell JR, Giggs RC. Inherited, metabolic, endocrine, and toxic myopathies. In: Isselbacher KJ, Braunwald E, Wilson JD, Martin JB, Fauci AS, Kasper DL (eds): Harrison' s principles of internal medicine, 13th edition. New York, McGraw-Hill, 1994, pp2385-2385.
3. Nguyen HH, Wolfe TJ III, Holmes DR Jr, et al: Pathology of the cardiac conduction system in myotonic dystrophy: a study of 12 cases. J Am Coll Cardiol 11: 662, 1988.
4. Hiromasa S, Ikeda T, Kubota K, et al: Ventricular tachycardia and sudden death in myotonic dystrophy. Am Heart J 115: 914, 1988.
5. Kurata C, Tawarahara K, Taguchi T, et al: Myocardial emission computed tomography with iodine-123-labeled beta-methyl-branched fatty acid in patients with hypertrophic cardiomyopathy. J Nucl Med 33: 6, 1992.
6. Tamaki N, Kawamoto M, Yonekura Y, et al: Regional metabolic abnormality in relation to perfusion and wall motion in patients with myocardial infarction: assessment with emission tomography using an iodinated branched fatty acid analog. J Nucl Med 33: 659, 1992.
7. Takeishi Y, Abe S, Tonooka I, et al: Heterogeneous myocardial distribution of iodine-123 15-(*p*-iodophenyl)-3-R, S-methylpentadecanoic acid (BMIPP) in patients with hypertrophic cardiomyopathy. Eur J Nucl Med 19: 775, 1992.
8. Franken PR, DeGeeter F, Dendale P, et al: Abnormal free fatty acid uptake in subacute myocardial infarction after coronary thrombolysis: correlation with wall motion and ionotropic reserve. J Nucl Med 35: 1758, 1994.
9. Nakjima K, Shimizu K, Taki J, et al: Utility of Iodine-123-BMIPP in the diagnosis of and follow-up of vasospastic angina. J Nucl Med 36: 1934, 1995.
10. Henderson EB, Kahn JK, Corbett JR, et al: Abnormal I-123 metaiodobenzylguanidine myocardial washout and distribution may reflect myocardial adrenergic derangement in patients with congestive cardiomyopathy. Circulation 78: 1192, 1988.
11. Stanton MS, Tuli MM, Radtke NL, et al: Regional sympathetic denervation after myocardial infarcton in humans detected noninvasively using I-123-metaiodobenzylguanidine. J Am Coll Cardiol 14: 1519, 1989.
12. McGhie AI, Corbett JR, Akers MS, et al: Regional cardiac adrenergic function using I-123 metaiodobenzylguanidine tomographic imaging after acute myocardial infarction. Am J Cardiol 67: 236, 1991.
13. Nakajima K, Shuke N, Nitta Y, et al: Comparison of ^{99m}Tc-pyrophosphate, ^{201}Tl perfusion, ^{123}I-lablled methyl-branched fatty acid and sympathetic imaging in acute coronary syndrome. Nucl Med Comm 16: 494, 1995.
14. Machida K, Honda N, Mamiya T, et al: Abnormal sympathetic innervation of the heart in a patient with myotonic dystrophy detected with I-123 MIBG cardiac SPECT. Clin Nucl Med 19: 968, 1994.
15. Pizutti A, Friedman DL, Caskey CT. The myotonic dystrophy gene. Arch Neurol 50: 1173, 1993.
16. Novelli G, Gennarelli M, Fattorini C, et al: The dynamics of myotonic dystrophy and its clnrical relevance: an overview. Biomed & Pharmacother 47: 321, 1993.
17. Buxton J, Shelbourne P, Davis J, et al: Detection of an unstable fragment of DNA specific to individuals with myotonic dystrophy. Nature 355: 547, 1992.
18. Merlet P, Valette H, Dubois-Randé JL, et al: Prognostic value of cardiac metaiodobenzylguanidine imaging in patients with heart failure. J Nucl Med 33: 471, 1992.
19. Gibson DG. Estimation of left ventricular size by echocardiography. Br Heart J 35: 128-132, 1972.

20. Brook JD, McCurrach ME, Harley HG, et al: Molecular basis of myotonic dystrophy. Expansion of a trinucleotide (CTG) repeat at the 3' end of a transcript encoding a protein kinase family member. Cell 68: 799, 1992.
21. Annane D, Duboc D, Mazoyer B, et al: Correlation between decreased myocardial glucose phosphorylation and the mutation size in myotonic dystrophy. Circulation 90: 2629, 1994.
22. Jansen G, Willems P, Coerwinkel M, et al: Gonosomal mosaicism in myotonic dystrophy patients: Involvement of mitotic events in (CTG)n repeat variation and selection against extreme expansion in sperm. Am J Hum Genet 54: 575, 1994.
23. Nakajyo M, Shimabukuro K, Miyaji N, et al: Rapid clearance of iodine-131 MIBG from the heart and liver of patients with adrenergic dysfunction and pheochromocytoma. J Nucl Med 26: 357, 1985.
24. Sisson JC, Shapiro B, Meyers L, et al: Metaiodobenzylguanidine to map scintigraphically the adrenergic nervous system in man. J Nucl Med 28: 1625, 1987.
25. Robinovitch MA, Rose CP, Schwab AJ, et al: A method of dynamic analysis of iodine-123-metaiodobenzylguanidine scintigrams in cardiac mechanical overload hypertrophy and failure. J Nucl Med 34: 589, 1993.
26. Imamura Y, Ando H, Mitsuoka W, et al: Iodine-123 metaiodobenzylguanidine images reflect intense myocardial adrenergic nervous activity in congestive heart failure independent of underlying cause. J Am Coll Cardiol 26: 1594, 1995.
27. Kinoshita M, Takahashi R, Hasegawa T,et al: $(CTG)_n$ expansions in various tissues from a myotonic dystrophy patient. Muscle & Nerve 19: 240, 1996.
28. Hawley RJ, Milner MR, Gottdiener JS, et al: Myotonic heart disease: A clinical follow-up. Neurology 41: 259, 1991.
29. Lerch H, Bartenstein P, Witcher T, et al: Sympathetic innervation of the left ventricle is impaired in arrhythmogenic right ventricular disease. Eur J Nucl Med 20: 207, 1993.
30. Witcher T, Hindricks G, Lerch H, et al: Regional myocardial sympathetic dysinnervation in arrhythmogenic right ventricular cardionryopathy. An analysis using ^{123}I-mata-iodobenzylguanidine scintigraphy. Circulation 89: 667, 1994.
31. Gill JS, Hunter GJ, Gane J, et al: Asymmetry of cardiac [^{123}I]meta-iodobenzylguanidine scans in patients with ventricular tachycardia and "clinically normal heart". Br Heart J 69: 6, 1993.
32. Müller KD, Jakob H, Neuzner J, et al: ^{123}I-metaiodobenzylguanidine scintigraphy in the detection of irregular regional sympathetic innervation in long QT syndrome. Eur Heart J ; 14: 316, 1993.
33. Shakespeare CF, Page CJ, O'Doherty MJ, et al: Regional sympathetic innervation of the heart by means of metaiodobenzylguanidine imaging in silent ischemia. Am Heart J 125: 1614, 1993.
34. Gill JS, Hunter GJ, Gane G, et al: Heterogeneity of the human myocardial sympathetic innervation: In vivo demonstration by iodine 123-labeled meta-iodobenzylguanidine scintigraphy. Am Heart J 126:390, 1993.
35. Tsuchimoti S, Tamaki N, Tadamura E, et al: Age and gender differences in normal myocardial adrenergic neural function evaluated by iodine-123-MIBG imaging. J Nucl Med 36:969, 1995.
36. Matsuo S, Takahashi M, Nakamura Y, et al: Evaluation of cardiac sympathetic innervation with iodihe-123-mretaiodobenzylguanidine imaging in silent myocardial ischemia. J Nucl Med 37: 712, 1996.
37. Germano G, Chua T, Kiat H, Areeda JS, et al: A quantitative phantom analysis of artifacts due to hepatic activity in technetium-99m myocardial perfusion SPECT studies. J Nucl Med 35: 356, 1994.